Ain Shams Engineering Journal (2014) 5, 553–568

Ain Shams University

Ain Shams Engineering Journal

www.elsevier.com/locate/asej
www.sciencedirect.com

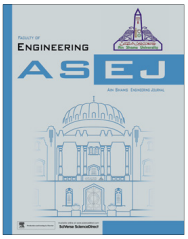

MECHANICAL ENGINEERING

Experimental studies on the effect of water contaminants in convective boiling heat transfer

Mohammad Mohsen Sarafraz *, **Faramarz Hormozi** [1]

Faculty of Chemical, Petroleum and Gas Engineering, Semnan University, Semnan, Iran

Received 23 June 2013; revised 11 October 2013; accepted 7 November 2013
Available online 28 December 2013

KEYWORDS

Water contaminants;
Flow boiling heat transfer;
Single-phase sub-cooling;
Vertical annulus

Abstract Experimental investigations on the influences of different contaminants to deionized water have been conducted under the sub-cooled flow boiling heat transfer inside the vertical annulus. Many experiments have been performed to investigate the influence of different operating parameters on the flow boiling heat transfer coefficient in the upward flow of contaminated water under the atmospheric pressure. The experimental apparatus provides the particular conditions to investigate the influence of heat flux (up to 132 kW/m^2), flow rate (1.5–3.5 l/min), sub-cooling level (Max. 30 °C), and concentration of contaminants (1–5% by volume). According to the results, with increasing the heat flux and flow rate, the flow boiling heat transfer coefficient and rate of bubble formation significantly increase. Results also demonstrated that adding contaminants to the deionized water causes the flow boiling heat transfer coefficient to be deteriorated. Likewise, sub-cooling level may only influence on the onset of nucleate boiling and heat flux corresponding to beginning of nucleate boiling phenomenon which is called inception heat flux.

1. Introduction

Flow boiling has long played a major role in many technological applications due to its superior heat transfer performance. Because of unknown sub-phenomena and mechanisms involved in the boiling phenomenon, many investigators have conducted many experiments to discover the complications and unknown properties of boiling processes. Boiling of impure liquids includes different components that are integrated with simultaneous heat and mass transfer between vapor inside the bubble and the vapor/liquid interface, which turns the phenomenon and its mechanisms much more complicated. In many industrial applications, contaminants may get mixed with pure water. This would influence on the heat transfer process and hence deteriorates the effectiveness of such applications. Contaminations may take place in many applications including heat exchangers, boilers, internal combustion engines, etc. In case of water to water heat exchangers, the pure water at high temperature may get mixed and contaminated with sea or river water due to leakage which may occur as a result of tube faults [1,2]. In car radiators, many contaminants

* Corresponding author. Tel.: +98 9166317313; fax: +98 6324231683.
E-mail addresses: mohamadmohsensarafraz@gmail.com (M.M. Sarafraz), fhormozi@semnan.ac.ir (F. Hormozi).
[1] Tel.: +98 9123930495.

Peer review under responsibility of Ain Shams University.

Production and hosting by Elsevier

2090-4479 © 2013 Production and hosting by Elsevier B.V. on behalf of Ain Shams University.
http://dx.doi.org/10.1016/j.asej.2013.11.006

Nomenclature

A	area, m^2
C_p	heat capacity, J/kg °C
d_h	hydraulic diameter, m
f	fanning friction number
ΔH	heat of vaporization, J/kg
k	thermal conductivity, W/m °C
l_{th}	heated length, m
L	length of annulus, m
P	pressure, Pa
q	heat, W
R	resistance, m^2 K/W or m^2 °C/W
Re	Reynolds number
T	temperature, K or °C
t	time, s

Subscripts and superscripts

c	critical
fb	flow boiling
in	inlet
out	outlet
l	liquid
m	mixture
nb	nucleate boiling
r	reduced
f	fouling
s	sub-cooled
th	thermocouples
v	vapor
w	wall

Greek symbols

α	heat transfer coefficient, W/m^2 K
δ	distance between thermocouple location and surface
ρ	density, kg/m^3
μ	viscosity, kg m/s
λ	thermal conductivity, W/m K
v	velocity, m/s

Dimensionless number

Re	Reynolds number, $\mathrm{Re} = \frac{\rho v d}{\mu}$
Pr	Prantdl number, $\mathrm{Pr} = \frac{Cp\mu}{k}$
Nu	Nusselt number, $\mathrm{Nu} = \frac{hx}{k}, x = \frac{d}{l}$

can be dissolved into the coolant fluid and change the quality of circulated fluid. In boilers, the total dissolved solids and other contaminants may get concentrated in the steam drum as a result of insufficient boiler blow down or other incidents [3]. In internal combustion engines, under many circumstances non-pure water may be added to the engine cooling system [4]. This is particularly true for military vehicles or vehicles used in non-urban areas. Also, sometimes the engine coolant becomes unpurified with some lube oil. In most of industrial heating tools which are cooling by a coolant fluid, sub-cooled flow boiling condition is observed. It means that the heated metal temperature is higher than the saturation temperature of coolant fluid, but the fluid bulk temperature is still lower than the saturation temperature, and the heat is transferred under the sub-cooled boiling conditions. However, more focus is given to the internal combustion engine applications as an elaborated example for the other applications considered in this work. In internal combustion engines improper coolants and inadequate cooling system maintenance can result not only in catastrophic overheating, but also in corrosion damage and even vessel flooding. Because most of the liquid cooling systems are difficult to observe, thus, damage can occur gradually over the time, essentially causing severe damage to the engine core. The cooling of an engine depends on the coolant properties [5,6], and the shape and geometry of cooling passages [7]. Engine coolants normally consist of a mix of water, anti-freeze, and different conditioners or inhibitors. Coolant must effectively remove heat, prevent freezing and resultant block damage, prevent deposits of scale and sludge on interior passages, inhibit corrosion, prevent cavitation erosion, lubricate components such as water pumps, and be compatible with hoses and seals [8]. Therefore, flow boiling has been one of the major concerns of investigators and a flash back to previous studies implies on this fact that there are many unknown aspects of boiling which currently are untouched that are briefly mentioned as follows: as an example of conducted researches, Zeitoun [9] performed a sub-cooled boiling test in a high heat flux condition; however, the test section for the boiling heat transfer was short in length and local bubble parameters were not provided. Early visualization experiments carried out by Hewitt et al. [10] showed that the bubbles affect the nucleation activity. The presence of moving bubbles leads to the wave-induced nucleation phenomenon observed by Barbosa et al. [11]. He conducted experiments in a vertical annulus in which heat was applied to the inner surface of the tube. A dominance of nucleate boiling was observed at low qualities. At high qualities, nucleate boiling was partly or totally suppressed and forced convection became the dominant mechanism. Thus, one may conclude that in internal flow boiling, the heat transfer coefficient is a combination of two mechanisms, nucleate boiling and forced convection. The heat transfer coefficient might remain constant, decrease or increase depending on the contribution of these two mechanisms during forced saturation boiling. Lee et al. [12] and Kim et al. [13] performed sub-cooled boiling experiments and analyzes the obtained results with CFD software. They truly distinguished the forced convection heat transfer mechanism from the nucleate boiling phenomenon. Sub-cooled flow boiling of heptane on both internally heated rod and resistance-heated coiled wire in an annular duct was examined by Muller-Steinhagen et al. [14]. Their results indicated that the boiling heat transfer coefficient increased with increasing heat flux but decreased with increasing system pressure and liquid sub-cooling, while independent of the mass velocity in the nucleate boiling regime. Hasan et al. [15] measured the sub-cooled nucleate boiling of R-113 flow in a vertical annulus, vertical annular channel and showed that

the boiling heat transfer coefficient was lower for higher pressure and sub-cooling. Moreover, the heat transfer coefficient increased with the mass velocity of the refrigerant flow. Sheikholeslami et al. [16] conducted experiments on sub-cooled flow boiling heat transfer of water–sugar mixture to show the effects of heat flux, fluid velocity, and sub-cooling on enhancing of nucleate boiling heat transfer in the partial flow boiling regime, where both forced convection and nucleate boiling heat transfer occurred. They found that increasing the sugar concentration led to a significant drop in the observed heat-transfer coefficient because of a mixture effect, which resulted in a local rise in the saturation temperature of sugar solution at the vapor–liquid interface. Peyghambarzadeh et al. [17] performed a large number of experiments to measure the heat transfer reduction and fouling resistance of $CaSO_4$ aqueous solutions in a vertical upward annulus under sub-cooled flow boiling condition. Experiments are designed so that the effects of different parameters such as solution concentration, wall temperatures, and heat flux as well as flow velocity on flow boiling heat transfer coefficient would be clarified. Ahmady et al. [18] conducted the experimental study of onset of sub-cooled annular flow boiling and surveyed the effect of pressure, mass flux, and inlet temperature of annulus on the inception heat flux. He illustrated that inlet temperature directly influences on the inception heat flux. Pavlenko and Lel [19] represented that at intensive boiling and evaporation of the falling liquid films, the presence of soluble admixtures (more high-temperature liquids) under the conditions of local dry spot formation leads to their intensive deposition on the heating surface. This significantly changes the capillary properties and increases thermal resistance. It was also found out that under evaporation conditions, admixtures are frozen out on the heating surface in the form of a thin film. At nucleate boiling, admixtures are intensively deposited in the region of complete liquid evaporation near the mobile dry spots in the form of separate solid particles with the size of 0.1–0.3 mm. Pecherkin et al. [20] and Volodin et al. [21] presented experimental investigation of heat transfer and critical heat flux at boiling and evaporation of falling films of liquid Freon mixtures. Experimental data on the effect of mixture concentration on heat transfer and on changes in the portion of low-boiling component along the falling film were collected at different heat flux and flow rate. It was shown that in the studied range of parameters, a change in mixture concentration does not lead to a change in heat transfer coefficient. Comparison of different predictive correlations for heat transfer coefficient and critical heat flux was also performed. Pavlenko et al. [22,23] conducted the experimental investigation on boiling and local heat transfer in the falling films of deionized water in sub-cooled condition. They used the high-speed thermo-graphic and video recording in their studies to record the temperature fields on the heating section surface and free surface of the falling film. The effect of liquid sub-cooling, heat flux and liquid flow rate on boiling of falling films was investigated and heat transfer coefficient of boiling of water was experimentally measured. For an extensive literature survey of flow boiling in conventional-size channels the reader is referred to Kew et al. [24,25] or for small-diameter channels to Kandlikar et al. [26,27], or Chen [28] and Bergles et al. [29]. Helali [30] investigated the effect of four different contaminants to pure water and expressed that adding any of the contaminants at all considered concentrations to distilled water impairs the heat transfer process substantially but he did not report any information about the range of Reynolds number, sub-cooling effect, data reduction and validation of experimental data. Moreover, no comparisons between predictive correlations and obtained data were carried out. These lacks of information determined us to evaluate the effect of three different contaminants on the sub-cooled flow boiling heat transfer inside the vertical annulus in an upward fluid flow.

In this paper, experimental investigation on the effect of different operating parameters on the flow boiling heat transfer coefficient of contaminated deionized water has been conducted. Influence of concentration of contaminants on the flow boiling heat transfer coefficient has experimentally been investigated and discussed. Interestingly, unlike the similar previous works, visual study on the bubble formation in nucleate boiling heat transfer area for different test mixtures have been carried out. Accordingly, Persian Gulf contaminated water, Caspian contaminated seawater and FC-ISO spindle oil (used in CNC machineries) has been employed as contaminants and was added into deionized water. As a data reduction and validation, a comparison between existing correlations and experimental data has been performed for deionized water. Scale formation and fouling resistance of contaminants were also experimentally and visually investigated.

2. Experimental

2.1. Experimental apparatus

Fig. 1 shows the test apparatus used for the present investigation. The liquid flows (by centrifugal pump manufactured by DAB CO.) in a closed loop consisting of temperature controlled storage tank, centrifugal pump and the annular test section. The flow velocity of the fluid was measured with calibrated Ultrasonic flow meter (manufactured by Flow-netix® Co.). The fluid temperature was measured by two PT-100 thermocouples installed in two thermo-well locators just before and after the annular section. The complete cylinder was made from stainless steel. Thermocouple voltages, current and voltage drop from the test heater were all measured and processed with a data acquisition system in conjunction with a PID temperature controller. Pressure drop of test section can also be measured using two pressure transmitter which is out of goals of this work. The test section shown in Fig. 2 consists of an electrically heated cylindrical DC bolt heater (manufactured by Cetal Co.) with a stainless steel surface, which is mounted concentrically within the surrounding pipe. The dimensions of the test section are: diameter of heating rod, 20 mm; annular gap diameter (hydraulic diameter) 30 mm; length of stainless steel rod, 300 mm; length of heated section, 140 mm and length of annulus 400 mm. Heat fluxes and wall temperatures can be as high as 1,320,000 W/m^2 and 150 °C, respectively. The local wall temperatures have been measured with four stainless steel sheathed K-type thermocouples which have been installed close to the heat transfer surface. The real wall temperature can be calculated from the following:

$$T_w = T_{th} - q\frac{s}{\lambda_w} \quad T_w = T_{th} - q''\delta/k \tag{1}$$

T_{th} is the arithmetic average of values of four thermocouples. The ratio between the distance of the thermocouples from

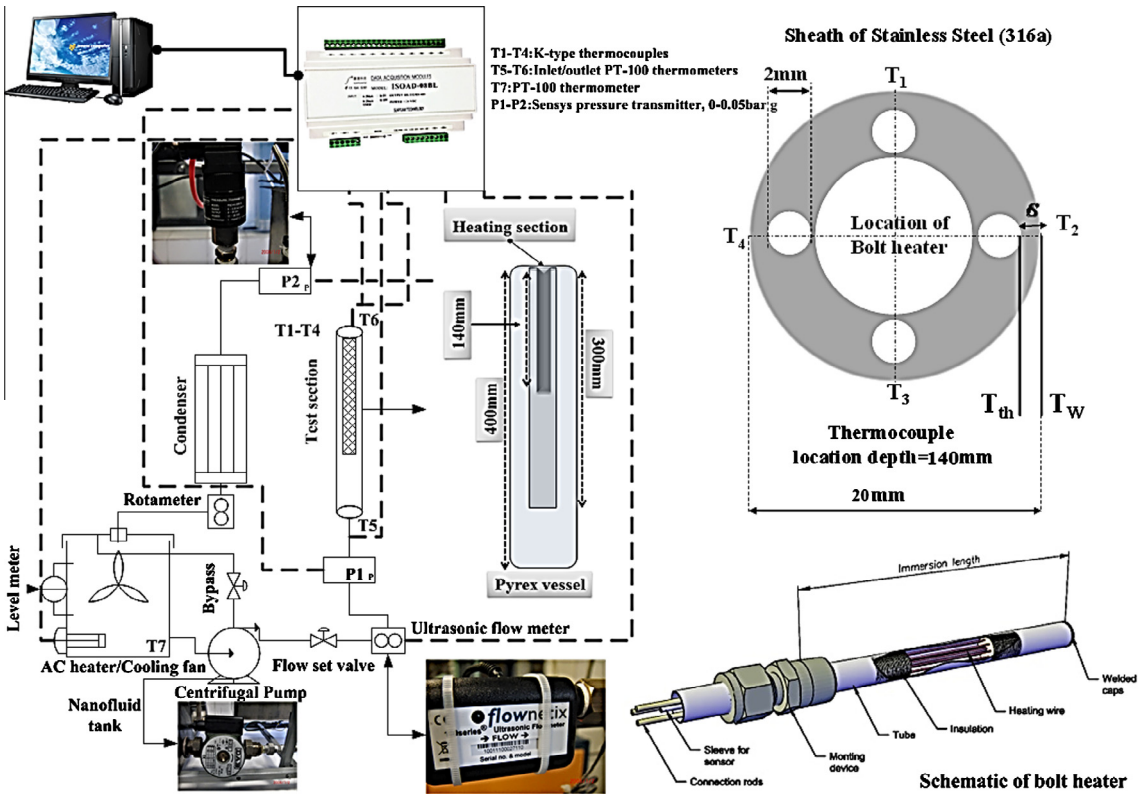

Figure 1 A scheme of experimental apparatus.

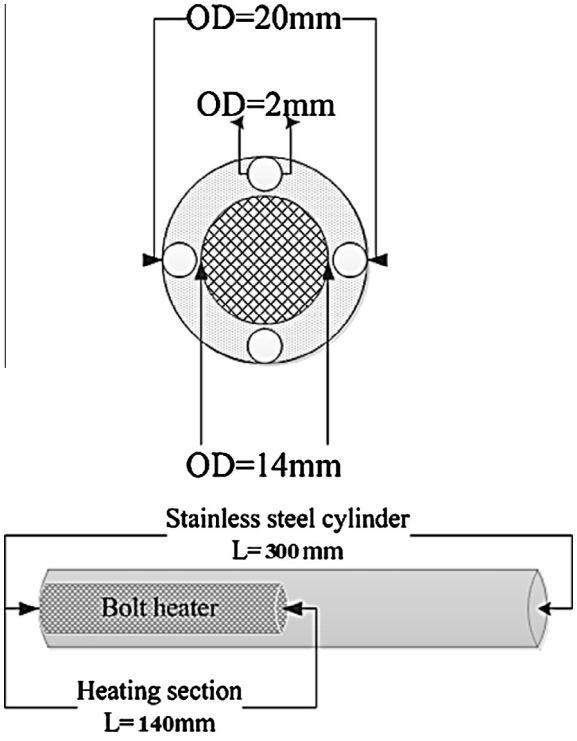

Figure 2 Details of annular space and heating section.

the surface (δ) and the thermal conductivity of the tube material, ($\frac{\delta}{k}$) was determined for each thermocouple by calibration measurements using a Wilson plot technique [31]. The average of 15 V readings was used to determine the difference between the wall and bulk temperature for each thermocouple. All the thermocouples were thoroughly calibrated by using a constant temperature water bath, and their accuracy has been estimated to $\pm 0.3K$. The local heat transfer coefficient α is then calculated from:

$$\alpha = \frac{q''}{T_w - T_s} \tag{2}$$

where T_s is the sub-cooled liquid temperature. To minimize the thermal contact resistance, high quality silicone paste was injected into the thermocouple wells. To avoid possible heat loss, main tank circumferences were heavily isolated using industrial wool glass. To control the fluctuations due to the alternative current, a regular DC power supply was also employed to supply the needed voltage to central heater. Likewise, to take the boiling photos, annulus was fabricated from the Pyrex, (thermo-resistant type of glass). More details of the test section and apparatus are given in Figs. 1 and 2.

2.2. Experiment procedure

Prior to commencing a test run, test heater, reservoir tanks and pipes were acid washed and cleaned to remove any scale from previous experiments. Once the system was cleaned, the test solution and the cleaning agent were introduced to the reservoir tanks. Following this, the tank heater was switched on and the temperature of the system increased. When the fluid had reached the desired temperature, the pump was started and the rig allowed to be stabilized at the desired bulk temper-

ature and velocity. Then, the power was supplied to the test heater and kept at a pre-determined value. The data acquisition system was switched on and temperatures, pressure and heat flux were recorded.

2.3. Error analysis

The uncertainties of the experimental results are analyzed by the procedures proposed by Kline and McClintock [32]. The method is based on careful specifications of the uncertainties in the various primary experimental measurements. The heat transfer coefficient can be obtained using Eq. (3):

$$\alpha = \frac{\rho V Cp(T_{out} - T_{in})}{(T_w - T_s)_{av.}} \tag{3}$$

T_s is the bulk sub-cooled temperature. As seen from Eq. (3), the uncertainty in the measurement of the heat transfer coefficient can be related to the errors in the measurements of volume flow rate, hydraulic diameter, and all the temperatures as follows.

$$\alpha = \lfloor fV, A_h, (T_{out} - T_{in}), (T_w - T_b) \rfloor \tag{4}$$

$$\partial\alpha = \sqrt{\left[\left(\frac{\partial\alpha}{\partial V}\right)\cdot\delta V\right]^2 + \left[\left(\frac{\partial\alpha}{\partial A}\right)\cdot\delta A\right]^2 + \left[\left(\frac{\partial\alpha}{\partial(T_{out}-T_{in})}\right)\cdot\delta(T_{out}-T_{in})\right]^2 + \left[\left(\frac{\partial\alpha}{\partial(T_w-T_b)}\right)\cdot\delta(T_w-T_b)\right]^2} \tag{5}$$

According to the above uncertainty analysis, the uncertainty in the measurement of the heat transfer coefficient is ±16.23%. The detailed results from the present uncertainty analysis for the experiments conducted here are summarized in Table 1. The main source of uncertainty is due to the temperature measurement and its related devices.

2.4. Physical properties of test liquids

Three different contaminants are considered to be added to the deionized water as the test mixture liquids in flow boiling heat transfer. Volumetric concentration of contaminant varies from 1% to 5%. For higher volume fractions of contaminants, the reported numerical values of physical properties are found to be inconsistent from different sources. In this work, unlike to the previous studies, all the physical properties have been calculated using standard correlations with known values of minimum expected uncertainty. The critical constants have been calculated using Joback method [33]. Expected uncertainty is reported equal to ±7 K (~±1%) for T_c; for P_c ±2 bar (~5%). Liquid density for test fluids has been calculated by Spencer and Danner [34] method with the maximum expected uncertainty of 7%. Liquid thermal conductivities for liquids had been predicted by methods summarized by Bruce et al. [35]. The expected uncertainties are reported less than 10% for pure liquids and up to 8% for liquid mixtures. Heat capacities for liquids have been calculated using Ruziicka and Domalski [36] method, with the expected uncertainty less than 4%. The heat capacities of liquid mixtures are estimated by mole fraction averages of the pure component values. Also results were analyzed by Atomic Absorption Device (Beijing Karaltay Scientific Instrument Co., Ltd., Model: PGI 990). Atomic Absorption Spectroscopy (AAS) is a spectro-analytical procedure for the quantitative determination of chemical elements employing the absorption of optical radiation (light) by free atoms in the gaseous state. In analytical chemistry the technique is used for determining the concentration of a particular element (analyte) in a sample to be analyzed. AAS can be used to determine over 70 different elements in solution or directly in solid samples. Table 2 represents the estimated physical properties of test fluids. Table 3 also shows the AAS test results for test liquids.

Note: characteristic of contaminants is selected such that can be compared to those of reported by Helali [30].

Table 1 Summary of the uncertainty analysis.

Parameter	Uncertainty
Length, width and thickness (m)	±0.00005
Temperature (K)	±0.3K
Fluid flow rate (l min^{-1})	±1.5% of readings
Voltage (V)	±1% of readings
Current (A)	±0.02% of readings
Cylinder side area (m^2)	$\pm 4\times10^{-8}$
Flow boiling heat transfer coefficient (W/m^2 K)	±16.235

2.5. Experimental data validation

To validate the experimental data, those of obtained results for deionized water (as a calibration fluid) have been compared to well-known modified Gnielinski correlation [37] for convective heat transfer region. Gnielinski proposed a correlation for predicting the forced convection heat transfer coefficient as follows:

$$\mathrm{Nu} = 0.86\cdot\left(\frac{d_i}{d_o}\right)^{-0.16}\cdot\left[\frac{\frac{f}{2}\cdot\mathrm{Re}\cdot\mathrm{Pr}}{1+12.7\sqrt{\frac{f}{8}}}\right]\cdot\left(1+\left(\frac{d_h}{L}\right)^{0.66}\right)\cdot\left(\frac{\mathrm{Pr}}{\mathrm{Pr}_{water}}\right)^{0.11} \tag{6}$$

Noticeably, Pr_w must be calculated in laminar condition and for the deionized water. Results of comparison demonstrate that the experimental data are in a good agreement with obtained results by the correlations with deviation of ±4.43%. To verify those of experimental data related to the region with nucleate boiling heat transfer dominant mechanism, Chen type model [28] has been employed. Results of this correlation ex-

Table 2 Physical properties of test liquids at temperature of 343 K.

Test fluids	Density (kg m^{-3})	Viscosity Pa s ($\times 10^3$)	Surface tension N/m ($\times 10^3$)	Heat capacity kJ/kg
Deionized water	997.43	1.0074	70.85	4.179
Persian Gulf water	1045	1.03	63.18	4.21
Khazar seawater	1154	1.07	61.28	4.319
Spindle oil water	1171	1.105	59.57	4.178

Table 3 Characteristic of water contaminants at temperature of 343 K.

Type	Deionized water	Persian Gulf water	Khazar seawater	Spindle oil water
PH	6.99–7.01	7.49	7.43	7.09
Electrical conductivity (mS)	0.0006	34.58	29.12	0.31
TDS (mg/l)	Undetermined	62,780	52,340	Undetermined
Na (mg/l)	0	19,643	17,893	0
K (mg/l)	0	86	798	Less than 0.001
Ca (mg/l)	Less than 0.001	998	712	Less than 0.001
Mg (mg/l)	Less than 0.001	2341	2124	Less than 0.001
CL (mg/l)	Less than 0.001	31,090	24,800	Less than 0.001
SO_4 (mg/l)	Less than 0.001	4541	4008	Less than 0.001
SiO_2 (mg/l)	Less than 0.001	12.09	8.004	Less than 0.001
Hardness $CaCO_3$ (mg/l)	5.1–8.87	71,103	6615	11.49–15.7

press the good agreement about ±6.98% with experimental data. Fig. 3 shows the result of comparison between experimental data related to flow boiling heat transfer coefficient of deionized water and well-known predictive correlations at different heat transfer regions.

As shown in Fig. 3, Gnielinski correlation is unable to predict the flow boiling heat transfer coefficient in nucleate boiling region but calculated results for convective heat transfer area are satisfying.

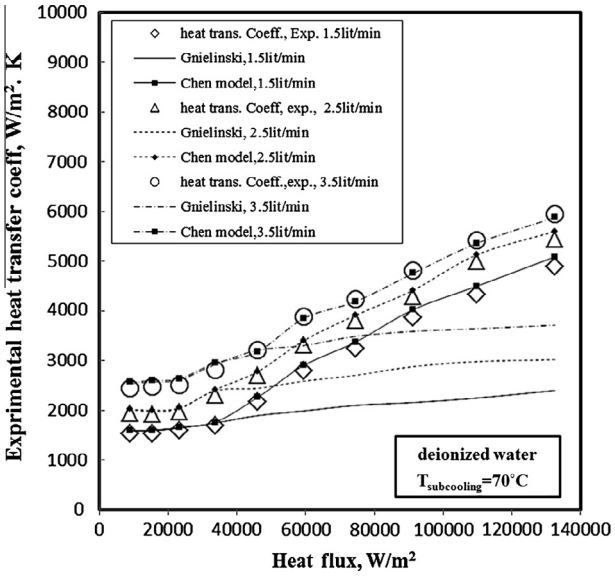

Figure 3 Results of comparisons between experimental data and well-known correlations.

3. Results and discussion

3.1. Effect of heat flux

The convenient style of demonstration of the effect of heat flux on the flow boiling heat transfer coefficient is in terms of heat flux versus flow boiling heat transfer coefficient directly. Experimental results demonstrated that heat flux is proportion to flow boiling heat transfer coefficient such that with increasing heat flux, the flow boiling heat transfer coefficient dramatically increases. For all three test fluids, with increasing the heat flux, heat transfer coefficient significantly increases. For

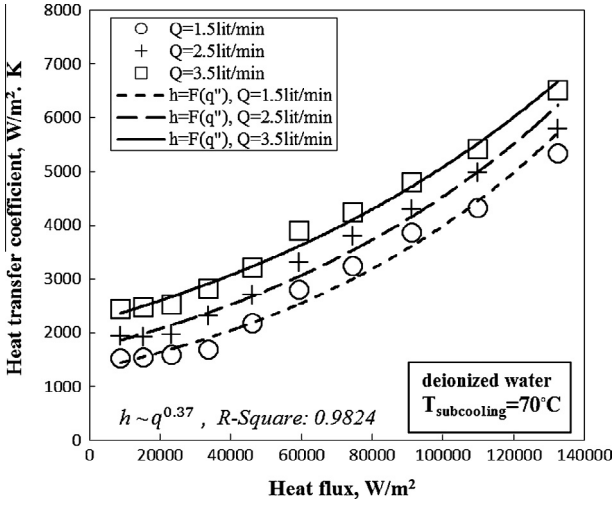

Figure 4 Effect of heat flux on the flow boiling heat transfer coefficient for deionized water.

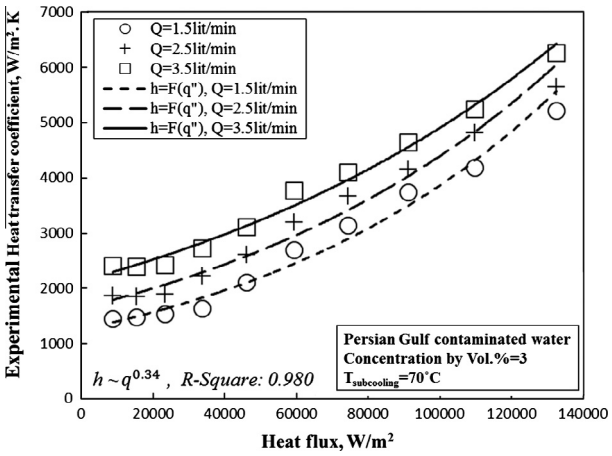

Figure 5 Effect of heat flux on the flow boiling heat transfer coefficient for contaminated Persian Gulf water (vol.% = 3).

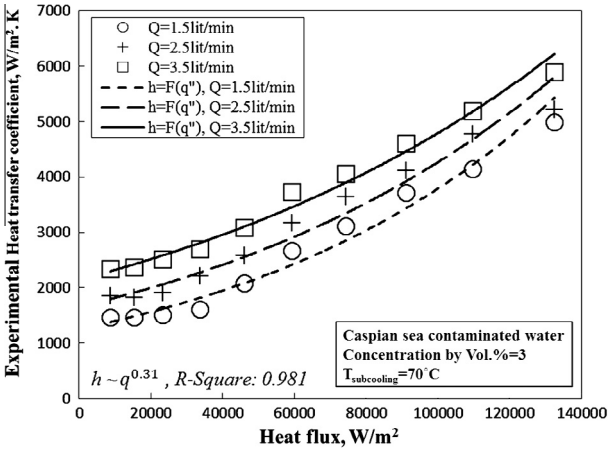

Figure 6 Effect of heat flux on the flow boiling heat transfer coefficient for contaminated Khazar sea (Caspian) water (vol.% = 3).

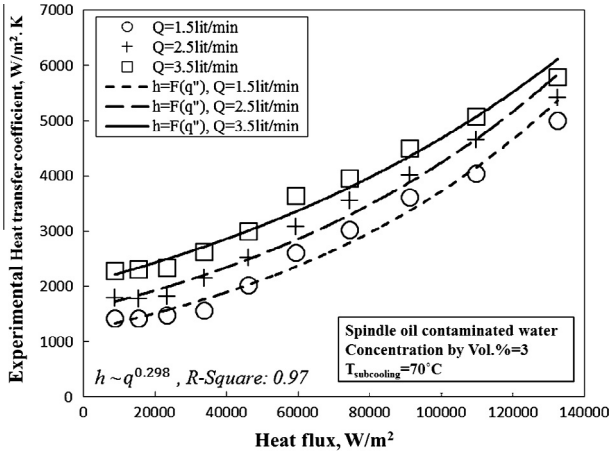

Figure 7 Effect of heat flux on the flow boiling heat transfer coefficient for contaminated spindle oil contaminated water (vol.% = 3).

better understanding, Figs 4–7 are depicted to represent the effect of heat flux on the flow boiling heat transfer coefficient of test fluids in comparison with deionized water at volumetric concentration of 3% (by volume) of contaminant. As shown, in lower heat fluxes (particularly in forced convection region), heat transfer coefficient slightly increases with increasing the heat flux (heat fluxes between 5000 and 40,000 W/m^2) and in this condition, flow boiling heat transfer coefficient can be considered as the independent of heat flux; however for nucleate boiling area, significant increase can be seen for all test fluids at any operating conditions.

To demonstrate the dependency of flow boiling heat transfer coefficient to heat flux, a simple mathematical interpolation has been employed that demonstrates an exponent proportion of heat transfer coefficient and heat flux for all three contaminants. Briefly speaking, result of interpolations express that flow boiling heat transfer coefficient is strictly depend to the heat flux with power variation range of $0.298 < n < 0.34$ with R-square of $0.98 > R^2 > 0.974$.

Figs. 5–7 typically depict the effect of heat flux on the flow boiling heat transfer coefficient for contaminated Persian Gulf, Khazar (Caspian) sea and spindle oil/water mixtures respectively.

Noticeably, for spindle oil contaminated water; lower exponential behavior relative to the heat flux can be seen in comparison with other contaminants. The major reason of this fact can be referred to different reasons which are fully explained in following sections of this work. Other reasons are namely: difficulty in estimating the physical properties of mixture due to the weakness of mixing rules, variation in surface tension and significant changes in viscosity of mixture and unpredictable molecular behavior of mixtures ones of the major problems facing with hydrocarbon mixtures. Among of the mentioned reasons, surface tension is a key parameter in nucleate boiling heat transfer and boiling subphenomena such as bubble formation and nucleation active sites. During the boiling heat transfer, concentration of micro-layer is constantly under the influence of surface temperature. Therefore, thermal properties of liquids around and inside the micro-layer are not constant, particularly, surface tension of liquid phase. Consequently, internal forces in micro-layer will change and subsequently balance of forces on the surface will change such that the wettability and contact angle of bubbles also changes. Then, heating surface is covered by bubbles and therefore, surface becomes thermal-isolated locally which leads the heat transfer to be deteriorated. However, the Marangoni effect plays a significant role in augmentation of the heat transfer which has not been reported in oils and high concentration hydrocarbons yet. The other reason is due to the presence of mass transfer due to the very higher vapor pressure of water in comparison with spindle oil at similar conditions. Accordingly, considering the saturation temperature of water and spindle oil, generated bubbles around the heated surface (boiling micro-layer) enrich of lighter component (water, no spindle oil is considered to evaporate) and thus, mass transfer driving force is expected between the interface of bubbles and bulk of liquid. During the bubble formation, in boiling of water–spindle mixture, a concentration gradient will be established through the vapor/liquid interface causing water to diffuse toward the gas–liquid interface and evaporates there, while oil to diffuse in the reverse direction toward the liquid bulk.

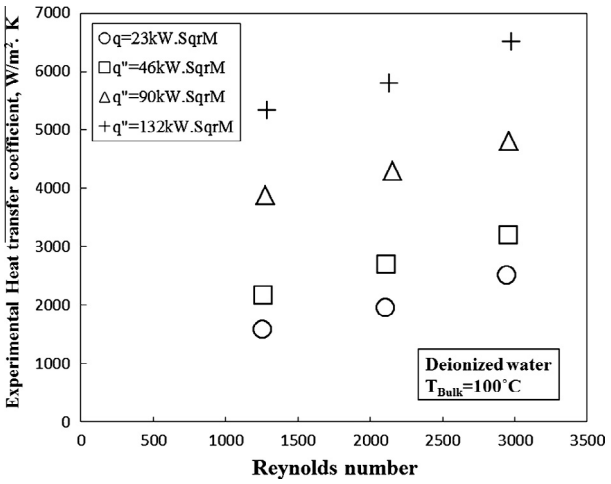

Figure 8 Effect of fluid flow rate (fluid velocity) on the flow boiling heat transfer coefficient for deionized water.

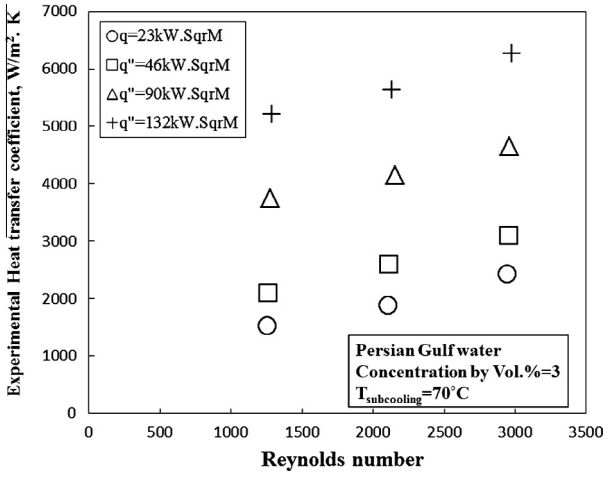

Figure 9 Effect of fluid flow rate (fluid velocity) on the flow boiling heat transfer coefficient for Persian Gulf contaminated water (vol.% = 3).

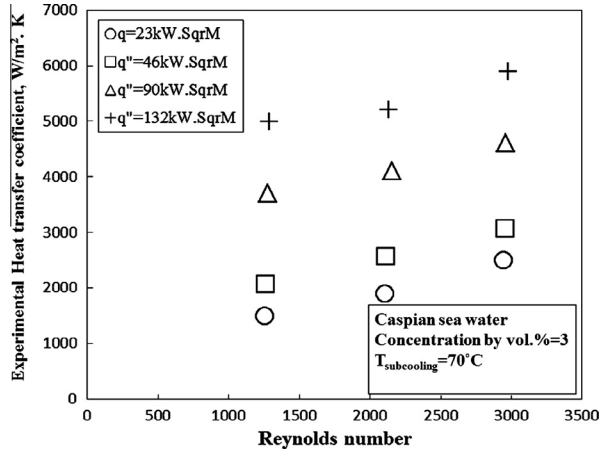

Figure 10 Effect of fluid flow rate (fluid velocity) on the flow boiling heat transfer coefficient for Khazar sea contaminated water (vol.% = 3).

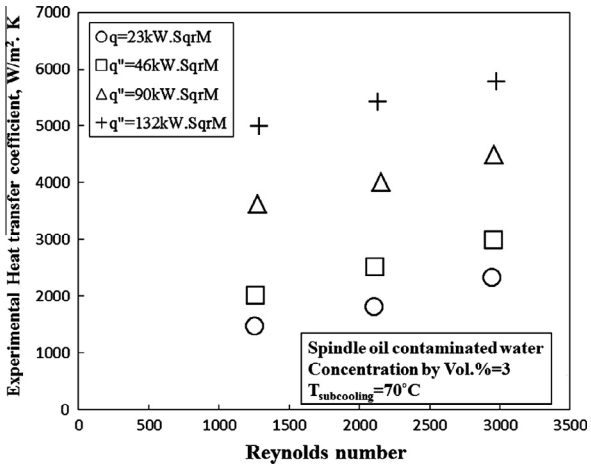

Figure 11 Effect of fluid flow rate (fluid velocity) on the flow boiling heat transfer coefficient for spindle oil contaminated water (vol.% = 3).

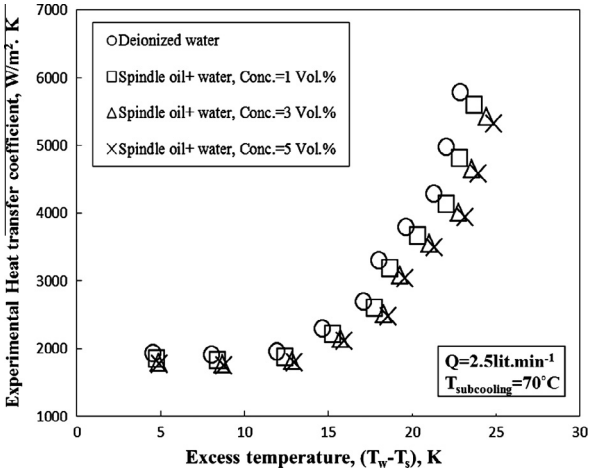

Figure 12 Effect of concentration of contaminants on the flow boiling heat transfer coefficient for deionized water and spindle oil.

However for other two contaminants physical properties are not change as much as that of changed for oil/water. A simple comparison between Tables 2 and 3 shows that only adding 5% of spindle oil to the deionized water changes the surface tension from 70.85 to 59.57.

3.2. Effect of fluid flow rate (fluid velocity)

Fluid flow rate has a strong effect on the flow boiling heat transfer coefficient. It is more convenient to show the effect of flow rate on the flow boiling heat transfer coefficient in terms of Reynolds number versus heat transfer coefficient. With increasing the flow rate, the heat transfer coefficient significantly increases. For all the test fluids, increase in flow boiling heat transfer coefficient can also be seen with increasing the fluid flow rate. Figs. 8–11 depict the effect of flow rate on the flow boiling heat transfer coefficient of the test mixtures.

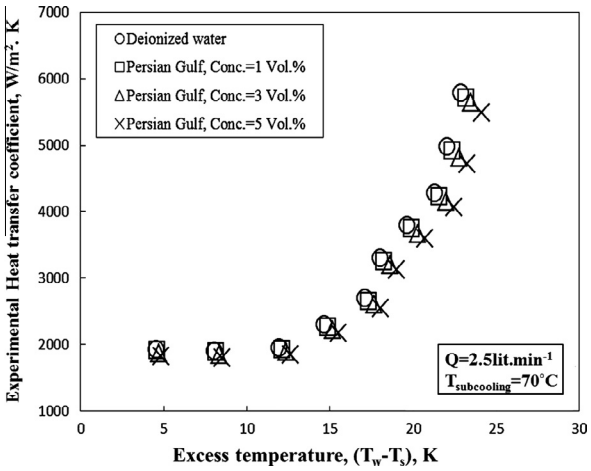

Figure 13 Effect of concentration of contaminants on the flow boiling heat transfer coefficient for deionized water and added Persian Gulf contaminated water.

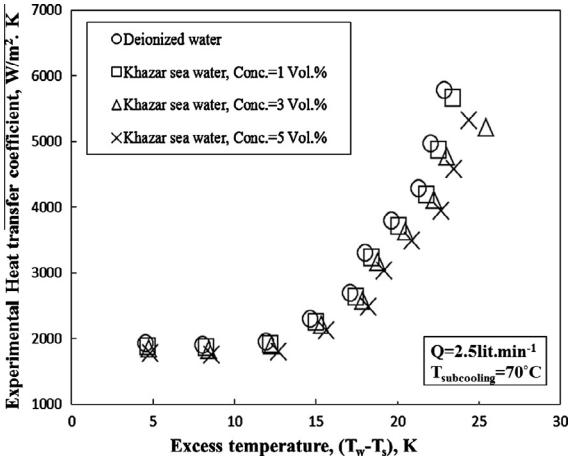

Figure 14 Effect of concentration of contaminants on the flow boiling heat transfer coefficient for deionized water and added Khazar sea contaminated water.

3.3. Effect of concentration of contaminant

Influence of concentration of contaminants on the flow boiling heat transfer coefficient at constant sub-cooling temperature of 70 °C and flow rate of 2.5 l/min and for the three test mixtures has been represented in Figs. 12–14. Fig. 12 shows the effect of volumetric concentration of spindle lube oil as a contaminant to the deionized water. Fig. 13 is typically representing the influence of increase in volumetric concentration of Persian Gulf contaminated water on the flow boiling heat transfer coefficient. Fig. 14 also shows the experimental results in case of using Khazar seawater as a contaminant. Comparisons have also been carried out to show the effect of concentration on test fluids and compared to those of results measured for deionized water.

It also can be found that with increasing the excess temperature (wall superheat temperature), higher boiling heat transfer coefficient can be seen, however with increasing the volumetric concentration of spindle oil heat transfer coefficient decreases. It can also be seen that increasing the oil concentration in the deionized water to 5% (by volume) in comparison with the pure state, caused the significant reduction in experimental flow boiling heat transfer coefficient. It can be concluded from the experimental data in Fig. 12 that using more spindle in the deionized water causes of a significant increase in wall superheat temperature. It can be also seen from the figure that at constant heat flux of 132 kW/m^2, the wall superheat was 22 °C for deionized water, while it increases to 25 °C when 5% of oil is added to the deionized water. Helali [30] reported the increase of 17 °C for 5% of lube oil added into distillated water for heat flux around 300 kW/m^2. Also at the same heat flux, adding 3% of oil caused the wall superheat to jump to only 24 °C. There are significant differences between experimental data obtained in this work and which Helali reported [30] which are owing to the different operating conditions of experiments such as maximum reachable heat flux and heater properties. Helali experimentally reached to the maximum heat flux of around 400 kW/m^2 while in this work the maximum reachable heat flux was 132 kW/m^2. Noticeably, in the present work, the major focus is on the low-moderate heat fluxes. Adding more spindle oil into the deionized water causes the wall to become hotter. Because, the boiling micro-layer around the heating surface becomes enricher of heavier component and the lighter component (water) is depleted slightly in micro-layer fluid around the surface. Therefore, bulk temperature around the surface and also the surface temperature increase. With considering the time, adding more oil creates a micro-layer of spindle oil around the heating surface that subsequently induces thermal resistance film on the heating surface and hence less heat transfer occurs. The less heat transfer through the metal, the higher wall temperature is reported and this may cause more thermal loading and thermal stresses which eventually may lead to metal cracks or failure in industrial heating tools [31]. Fig. 13 shows the experimental data related to the flow boiling heat transfer coefficient when Persian Gulf contaminated water is added to the deionized water in the rig.

It can be seen from the figure that adding 1%, 3% and 5% of Persian Gulf water deteriorates the heat transfer coefficient. To interpret the reasons for deterioration of heat transfer in boiling of mixtures, it can be said that the sub-cooled flow boiling is combined of two heat transfer mechanisms:

i. The heat transfer region with the forced convection dominant mechanism.
ii. The heat transfer area with nucleate flow boiling as a dominant heat transfer mechanism.

When Persian Gulf and other contaminants are added into the deionized water, reduction in heat transfer coefficient in forced convective and nucleate boiling regions is observed. Exact reasons for the deterioration of heat transfer are due to the:

(1) Reduction in temperature driving force because of increase in the boiling point of the micro-layer (the liquid layer trapped under a growing bubble) which is due to the preferential evaporation of the light components during bubble growth.
(2) The mass diffusion of the light components to the micro-layer (caused by the preferential evaporation) which is much slower than the heat transfer.

(3) The fact that there is usually a significant and non-linear variation in the mixture physical properties with composition and.
(4) The effect of composition on nucleation itself and scale formation as well as coating.

As another reason for reduction in heat transfer coefficient, according to the Stephan–Abdelsalam [38] and Gorenflo correlations [39], higher viscosity and surface tension of a component leads to the lower nucleate boiling heat transfer coefficient. Hence, this can be considered as another reason for deterioration of heat transfer in boiling of mixtures. Regarding to Table 2, heat transfer deterioration can be considered as: spindle oil $\gg$ Caspian seawater > Persian Gulf contaminated water. As represented in Table 3, Persian Gulf water contains relatively higher amounts of total dissolved solids (TDS), sodium (Na), sulfate (SO_4) and hardness ($CaCO_3$) in comparison with the contaminated Caspian seawater. Increasing the amounts of these substances seems to reduce the heat transfer due to the solids formed in the cooling water. Forming more sodium chloride salt (sodium and chlorine) in the water also causes considerable heat transfer barrier on the metal surface. Fig. 14 illustrates the effect of using seawater as a contaminant to the deionized water with concentration of 1%, 3% and 5% [31].

As shown in Fig. 14, adding Khazar seawater also deteriorates the heat transfer process as the wall superheat becomes higher when more seawater is added. Thus, seawater can be considered as relatively worse cooling fluid as it contains very high amounts of many solid and other substances although lower than Persian Gulf water as seen in Table 2. Seawater contains huge amount of TDS (52,340 mg/l) as well as chlorine and sodium, sulfate (SO_4), silicon oxide (SiO_2) and hardness. These substances form a thin insulating layer on the heat transfer surface and gives worse cooling to the metal. In fact existence of a coating of impurities around the heated surface dramatically reduces the heat transfer rate and subsequently impurity coating acts as insulation. Briefly speaking, the wall superheat for all contaminants added at all concentrations appears to have increased when compared to deionized water and subsequently, deterioration of heat transfer coefficient is reported for all three contaminants.

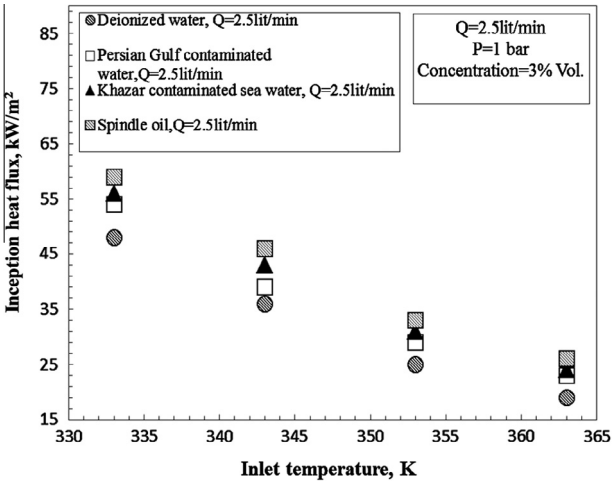

Figure 15 Effect of inlet temperature (sub-cooling effect) on the ONB inception heat flux.

3.4. Effect of sub-cooling (inlet temperature of annulus)

The outstanding influence of the inlet temperature of annulus, sub-cooling, can be seen on the inception heat flux. In fact, inception heat flux is defined as the heat flux in which the nucleate boiling begins. According to the experimental data, when sub-cooling increases (by decreasing the inlet temperature), the inception heat flux is shifted forward to the higher heat fluxes. Briefly speaking, higher sub-cooling causes a significantly time delay between formation of convective and nucleate boiling regions meaning that at higher heat fluxes, area related to convective zone is extended and the first generated bubbles may be seen at higher heat fluxes with significant time delay. In fact, with increasing the inlet temperature, inception heat flux decreases. Inception heat flux for spindle oil was the highest and: Inception heat flux can be ordered as follows: spindle oil > Caspian sea > Persian Gulf. In brief, the higher sub-cooling, the higher inception heat flux is reported. Although more studies and analysis is needed to specify the exact influence of inception heat flux on onset of nucleate boiling and flow boiling heat transfer coefficient which is out of goals of this research. Fig. 15 typically represents the inception heat fluxes or ONB (Onset of Nucleate Boiling) points for different sub-cooling levels for deionized water and other contaminants at 3% volumetric concentration of each contaminant.

Figure 16 Bubble formation at heat flux (a) 45 kW/m^2, (b) 54 kW/m^2, (c) 63 kW/m^2, (d) 91 kW/m^2, (e) 110 kW/m^2, and (f) 132 kW/m^2.

Fig 16. *(continued)*

Fig 16. *(continued)*

Fig 16. *(continued)*

Fig 16. *(continued)*

3.5. Bubble formation

Bubble formation is considered as a one of the important study branches of boiling sub-phenomena. Owing to the interactions of bubbles, unknown properties of surface when bubbles departure and physical properties of bubbly flow (as two phase flow) and nucleation active sites, many aspects of boiling phenomena is still untouched. In this work, experimental setup provides the particular conditions to capture that bubble formation and their interactions. The glass-made annuli provide the appropriate condition for taking photos to analyze the effect of operation parameters on the bubble formations. Nikon D90 DSLR camera was used as the image recorder. The camera was equipped with a SB-900 Speed light and a Nikkor. 18–105 mm-F3.5–5.5 zoom lens. The typical photo

Fig 16. *(continued)*

Fig 17. *(continued)*

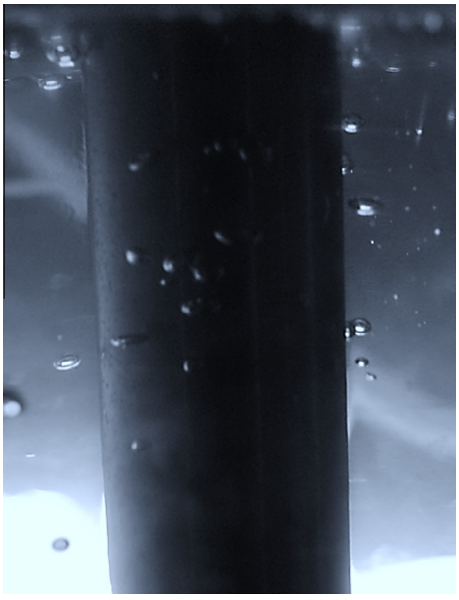

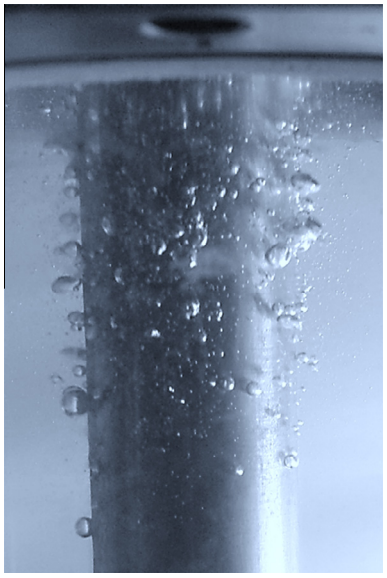

Fig 17. *(continued)*

Figure 17 Bubble formation at flow rate (a) 3.5 l/min, (b) 3 l/min, (c) 2.5 l/min, (d) 2 l/min, (e) 1.5 l/min, and (f) 1 l/min.

characteristics were: shutter speed: 1:1000s, ISO: 800, F: 5.5 and focal length: 100 mm (Approx.). Although these facility is not enough to predict the bubble mean diameter, but bubble formation can visually be studied through the taken photos. The results of visual experiments demonstrate that the bubble diameters increase with increasing heat flux; however, the impact of concentration seems to be complicated and cannot be investigated with such recording facilities. Fig. 16 illustrates the effect of heat flux on the rate of bubble formation for deionized water.

Visual results also demonstrated that fluid flow rate has a strong effect on bubble formation and bubble size. Increasing the flow rate of test fluid decreases the bubble size and also decreases the bubble formation. It is due to this reason that when flow rate of fluid increases, times for the formation of bubbles decreases meaning that dissolved vapor phase have not enough time to diffuse into the bubbles and due to the velocity of fluid bubbles departure the surface quicker and therefore, time is not enough for bubbles to be formed or grow. Fig. 17 represents the influence of fluid flow rate on the bubble formation

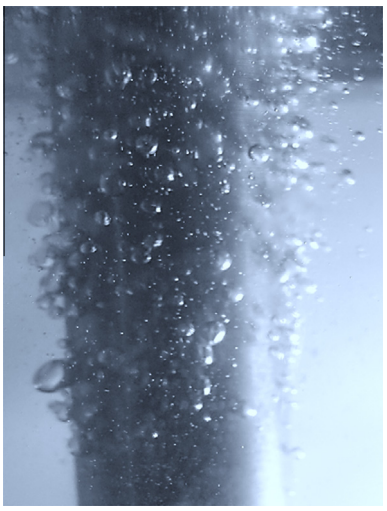

Fig 17. *(continued)*

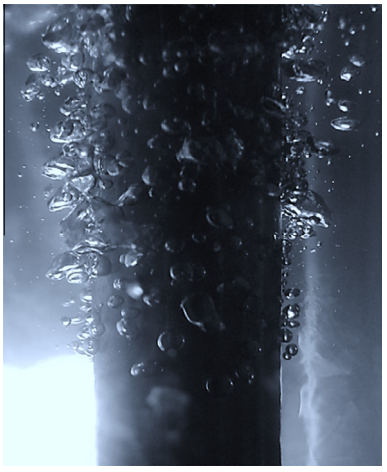

Fig 17. *(continued)*

of deionized water under the sub-cooled flow boiling heat transfer.

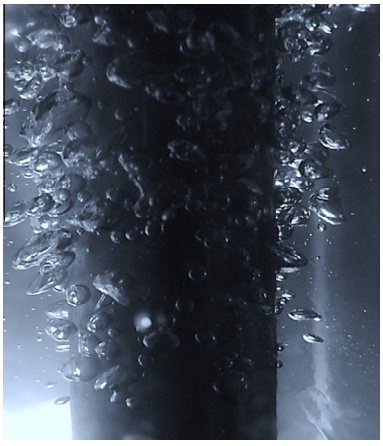

Fig 17. *(continued)*

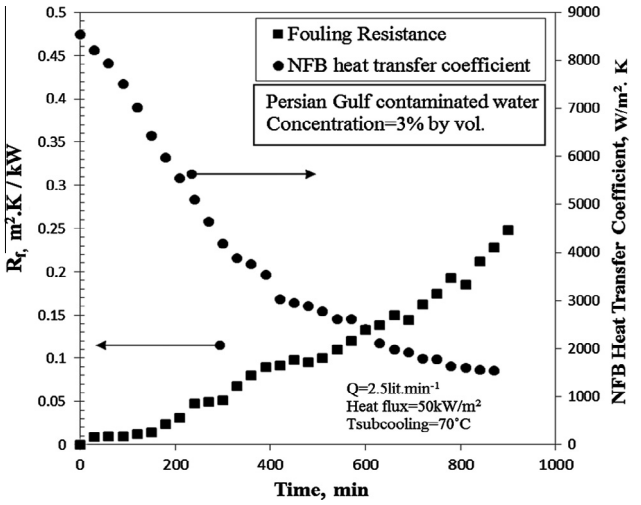

Figure 18 Fouling resistance and heat transfer coefficient of Persian Gulf contaminated water at given operating conditions.

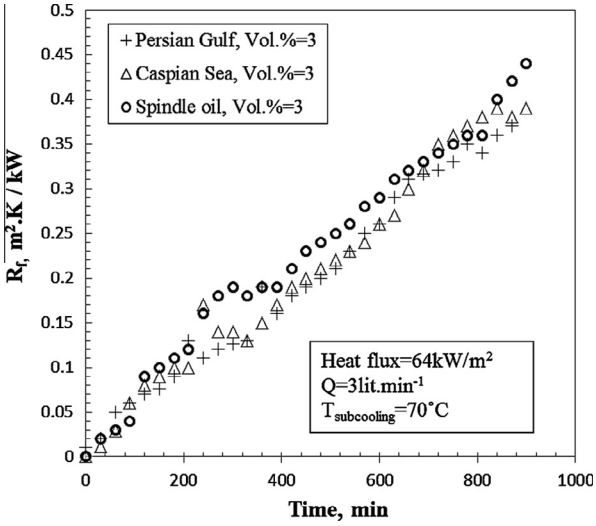

Figure 19 Experimental fouling resistances of different contaminants.

3.6. Influence of scale formation and sedimentation of impurities (contaminants)

A large number of experiments were performed to measure the fouling resistance of contaminated water around the vertical stainless steel cylinder inside the annular duct, however, in the present work. It is briefly discussed because; it is out of goals of this paper and is still undergone. It is customary to present fouling data in terms of fouling resistance (R_f) which can be calculated on the basis of heat transfer [40]:

$$R_f = \frac{1}{\alpha(t)} - \frac{1}{\alpha(t=0)} \tag{7}$$

Fig. 18 shows changes of flow boiling heat transfer coefficient and fouling resistance with time. As shown in Fig. 18, sub-cooled flow boiling heat transfer coefficient decreases with time due to the deposition of contaminants on the heat transfer

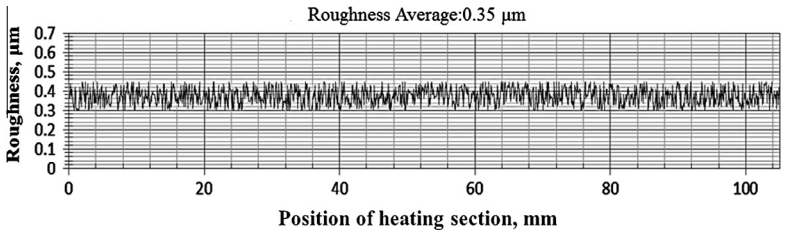

Figure 20 Surface roughness of heating section provided by Profile meter.

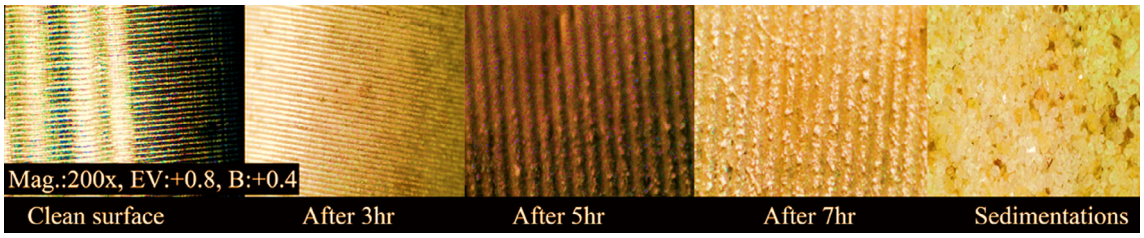

Figure 21 Scale formation of Persian Gulf contaminated water on the heating section at different period of time.

surface. Because, these contaminants cover the heating surface and slightly change the thermal resistance of surface. On the other hand, according to previous studies, microcavity and wettability of surface change and number of nucleation cavities dramatically increases and consequently, rate of bubble formation increases and as a result, more bubbles cover the heating section and lead to the heat transfer rate decreases. Experimental results reveal a rectilinear increase in fouling resistance with time which is a result of sedimentation fouling. Walker et al. [42] reported an asymptotic behavior of fouling resistance which may be attributed to additional particulate fouling. Peyghambarzadeh et al. [41] showed that the fouling resistance at the initial stages of the test period decreases even hit the negative value at some points. He expressed that this phenomenon may be due to the fact that during the nucleation stage, the nuclei forming on the heat transfer surface increases the surface roughness. This leads to an increase in the rate of heat transfer in comparison with clean surface heat transfer rate, thereby portraying the fouling resistance as negative. However, in the present work, no negative value of fouling resistance is reported.

Fig. 19 also depicts the experimental data related to the experimental fouling resistance as a function of time for different contaminants. Noticeably, other operating conditions such as temperature and concentration remained constant. The experimental data in Fig. 19 demonstrates that for the spindle oil, higher fouling resistance can be observed while the lowest fouling resistance can be seen for Persian Gulf contaminated water. In fact, at any other heat fluxes and fluid flow rates, linear behavior of fouling resistance for all the contaminants can be seen. Noticeably, before running the experiments, roughness of surface was measured using profile meter (Elcometer 7061 MarSurf PS1 Surface Roughness Tester) which is shown in Fig. 20. According to measured results, average roughness of surface was 0.35 μm which increased with time. After 3 h, 5 h and 7 h, measured roughness was 0.45, 58, 84 μm respectively. Study of the scale formation of water contaminants (in details) is undergone by our heat transfer research center in Semnan. Fig. 21 also shows the deposited layer of Persian Gulf contaminated water on the heating surface. Image has been taken using dnt® digital microscope with 200× power magnification at Semnan University (at following settings: excess voltage: +0.8, brightness: +0.4, backlight code: 0).

4. Conclusions

Experimental investigations on the effect of operation parameters and concentration of contaminants on three different contaminated water test fluids were performed and following conclusions have been made:

- The best heat transfer performance for all the operation parameters can be seen for the deionized water. In fact, during the boiling of deionized water no particulate or crystallization fouling can be seen around the heating surface and therefore, lower film thermal resistance of heating surface leads to the lower wall superheat temperature can be seen and consequently, higher heat transfer coefficient is reported. However, other parameters such as conditions of nucleation active sites, surface tension and mixture effects and local mass transfer due to the concentration driving force are other reason of deterioration of heat transfer coefficient for contaminated water.
- For all three contaminants as well as deionized water, heat flux has a direct effect on the flow boiling heat transfer coefficient. With increasing the heat flux, flow boiling heat transfer coefficient significantly increases. Likewise, for bubble diameter and rate of bubble formation, with increasing the heat flux, both of them dramatically increases.
- Fluid flow rate has a strong influence on the flow boiling heat transfer. With increasing the flow rate of fluid, mass velocity and subsequently heat transfer coefficient dramatically increases due to the local agitations around the heating surface and local reduction in wall temperature of heating surface. But in contrast, increasing the fluid flow rate reduces the bubble formation. Because, with increase in velocity of fluid, time for formation of bubble decreases

and subsequently diffusion of dissolved vapor phase into bubbles does not occur completely and therefore, bubbles does not have enough time to reach to their maximum size and leaves the heating surface sooner.

- For all concentration of contaminants added to the deionized water, deterioration of heat transfer coefficient can be observed. This phenomenon is mainly due to the coating constituted around the heating surface. For spindle oil a micro-layer of hydrocarbon appears around the circumference of heating surface and therefore, wall super heat temperature increases. Hence, lower flow boiling heat transfer coefficient is reported.
- At any heat fluxes, with increasing the concentration of contaminants, higher deterioration of heat transfer can be seen.
- The only effect of sub-cooling parameter can be seen on the inception heat flux. In fact, with increasing the fluid inlet temperature of annuli (decrease in sub-cooling level) inception heat fluxes reduce and shift down to the lower heat fluxes. Although, further analysis of the effect of inlet temperature on ONB for different contaminates is needed, as well as the boiling heat transfer performance.
- Results showed that fouling resistance of contaminated mixtures is a strong function of time and with increase the time, as expected, fouling resistance increases. Also, rectilinear behavior of fouling resistance was observed for all the three contaminants which can help to investigators who are engaged with modeling of particulate fouling. Results also showed that spindle oil represents the higher fouling resistance and lower flow boiling heat transfer coefficient.
- To predict the flow boiling heat transfer coefficient of contaminated water, a comparison between existing correlations and experimental data seems to be considered and if needed, a new correlation must be proposed. Utilization of this work can be applied to the industrial cooling systems, car radiators, refinery re-boilers and ship engine cooling systems.

Acknowledgments

We tend to appreciate Khorramshahr marine sciences and Technology University for their material and experimental supports. Also, special thanks to Semnan state University for their experimental facilities particularly imaging systems. We also tend to dedicate this work to the Imam Mahdi.

References

[1] Muller-Steinhagen H. Cooling-water fouling in heat exchangers. Adv Heat Transfer 1999;33:415–96.
[2] Dooley RB, Ball M, Bursik A, Rziha M, Svoboda R. Water chemistry in commercial water-steam cycles. Aqueous Syst Elev Temp Press 2004:677–716.
[3] Richard P, Beach WM. Apparatus and method for filtering used engine coolant. J Cleaner Prod 1997;5:252.
[4] Selim MYE, Helali AHB. Effect of coolant additives on thermal loading of diesel engine. Proc Inst Mech Eng, Part D J Automob Eng 2001;215:1131–42.
[5] Selim MYE, Helali AB, Elfeky S. Enhancement of coolant side heat transfer in water cooled engines by using finned cylinder heads. In: Proceedings of the ASME ICE division fall conference, Ottawa, Canada; 2005.
[6] Abou-Ziyan HZ. Forced convection and subcooled flow boiling heat transfer in asymmetrically heated ducts of T-section. Energy Convers Manage 2004;45:1043–65.
[7] Huang KD, Tzeng S, Ma W. Effects of anti-freeze concentration in the engine coolant on the cavitation temperature of a water pump. Appl Energy 2004;79:261–73.
[8] Song G, John StD. Corrosion behavior of magnesium in ethylene glycol. Corros Sci 2004;46:1381–99.
[9] Zeitoun O. Subcooled flow boiling and condensation. Ph.D. thesis. McMaster University, Canada; 1994.
[10] Hewitt GF, Kersey HA, Lacey PMC, Pulling DJ. Burnout and nucleation in climbing film flow. Int J Heat Mass Transfer 1965;8:793–814.
[11] Barbosa JR, Hewitt GF, Richardson SM. High-speed visualization of nucleate boiling in vertical annular flow. Int J Heat Mass Transfer 2003;46:5153–60.
[12] Lee TH, Park GC, Lee DJ. Local flow characteristics of subcooled boiling flow of water in a vertical concentric annulus. Int J Multi-phase Flow 2002;28(8):1351–68.
[13] Kim MO, Kim SJ, Park GC. The assessment of sub-cooled boiling models at low pressure. In: Proceedings of the 5th international conference on multiphase flow (ICMF'04), May 30–June 4, Yokohama, Japan; 2004.
[14] Muller-Steinhagen H, Watkinson AP, Epstein N. Sub-cooled-boiling and convective heat transfer to heptane flowing inside an annulus and past a coiled wire. Part I: experimental results. ASME J Heat Transfer 1986;108:922–7.
[15] Hasan A, Roy RP, Kalra SP. Experiments on sub-cooled flow boiling heat transfer in a vertical annular channel. Int J Heat Mass Transfer 1990;33:2285–93.
[16] You H, Sheikholeslami R, Doherty WOS. Flow boiling heat transfer of water and sugar solutions in an annulus, vol. 50(6). Wiley InterScience; 2004. p. 1119–28.
[17] Peyghambarzadeh SM, Vatani A, Jamialahmadi M. Application of asymptotic model for the prediction of fouling rate of calcium sulfate under sub-cooled flow boiling. Appl Therm Eng 2012;39:105–13.
[18] Ahmadi R, Nouri-Borujerdi A, Jafari J, Tabatabaei I. Experimental study of onset of sub-cooled annular flow boiling. Prog Nucl Energy 2009;51:361–5.
[19] Pavlenko AN, Lel VV. Heat transfer and crisis phenomena in a falling films of cryogenic liquid. Russ J Eng Thermophys 1997;7:177–210.
[20] Pecherkin NI, Pavlenko AN, Volodin OA. Heat transfer and crisis phenomena at boiling in the falling films of freons on the smooth and structured surfaces. Thermo-phys Aeromech 2012;19:143–54.
[21] Pecherkin NI, Pavlenko AN, Volodin OA. Flow dynamics, heat transfer and crisis phenomena in the films of binary freon mixtures, falling over the structured surface. Int J Fluid Mech Res 2012;39:125–35.
[22] Pavlenko AN, Surtaev AS, Tsoi AN. Transient heat transfer and development of crisis phenomena in falling liquid films at non-steady heat generation. In: Proc. of the ECI 8th intern. conference on boiling and condensation heat transfer, Switzerland, Lausanne; 2012.
[23] Pavlenko AN, Koverda VP, Reshetnikov AV, Surtaev AS, Tsoi AN, Mazheiko NA, Busov KA, Skokov VN. Disintegration of flows of superheated liquid films and jets. J Eng Thermophys 2013;22:3 174–193.
[24] Kew PA, Cornwell K. Correlations for the prediction of boiling heat transfer in small-diameter channels. Appl Therm Eng 1997;17:705–15.
[25] Lin S, Kew PA, Cornwell K. Two-phase heat transfer to a refrigerant in a 1 mm diameter tube. Int J Refrig 2001;24(1):51–6.
[26] Kandlikar SG, Grande WJ. Evolution of micro channel flow passages – thermo hydraulic performance and fabrication technology. Heat Transfer Eng 2003;24(1):3–17.

[27] Kandlikar SG. Boiling heat-transfer with binary-mixtures; low boiling in plain tubes. ASME J Heat Transfer 1998;120:388–94.
[28] Chen JC. A correlation for boiling heat transfer to saturated fluids in convective flow. Ind Eng Chem Process Des Dev 1966;5(3):322–9.
[29] Bergles AE, Lienhard VJH, Kendall GE, Griffith P. Boiling and evaporation in small diameter channels. Heat Transfer Eng 2003;24:18–40.
[30] Helali AB. Effects of water contamination on sub-cooled flow boiling heat transfer. Energy Convers Manage 2011;52:2288–95.
[31] Seara JF, Uhia FJ, Sieres J. Laboratory practices with the Wilson plot method. Exp Heat Transfer 2007;20:123–35.
[32] Kline SJ, McClintock FA. Describing uncertainties in single-sample experiments. Mech Eng 1953;75(1):3–12.
[33] Joback KG. M.S. Thesis in Chemical Engineering. Massachusetts Institute of Technology, Cambridge, Mass; 1984.
[34] Spencer CF, Danner RP. Improved equation for prediction of saturated liquid density. J Chem Eng Data 1972;17(2):236–41.
[35] Bruce E, Poling J, Prausnitz M, O'Connell JP. The properties of gases and liquids. 5th ed. New York: The McGraw-Hill Companies; 2004. p. 10-1–10-70.
[36] Ruzicka V, Domalski ES. Estimation of the heat-capacities of organic liquids as a function of temperature using group additivity. Compounds of carbon, hydrogen, halogens, nitrogen, oxygen, and sulfur. J Phys Chem Ref Data 1993;22:619–57.
[37] Gnielinski V. Wärmeübertragung in Rohren. VDI Wärme atlas. Düsseldorf: VDI-Verlag; 1986.
[38] Stephan K, Abdelsalam K. Heat transfer correlation for natural convection boiling. Int J Heat Mass Transfer 1980;23:73–87.
[39] Gorenflo D. Pool boiling. In: VDI heat atlas; 1993.
[40] Sarafraz MM, Hormozi F. Scale formation and subcooled flow boiling heat transfer of CuO–water nanofluid inside the vertical annulus. Exp Therm Fluid Sci 2013, http://dx.doi.org/10.1016/j.expthermflusci.2013.09.012.
[41] Peyghambarzadeh SM, Vatani A, Jamialahmadi M. Application of asymptotic model for the prediction of fouling rate of calcium sulfate under sub-cooled flow boiling. Appl Therm Eng 2012;39:105–13.
[42] Walker P, Sheikholeslami R. Assessment of the effect of velocity and residence time in $CaSO_4$ precipitating flow reaction. Chem Eng Sci 2003;58:3807–16.

M.M. Sarafraz is currently a Ph.D. student in Semnan state university, Semnan, Iran. He has published more than 23 scientific articles in international publications including the Elsevier, Taylor and Francis, Springer and Scopus. His research interests cover: nano/microfluid thermo-physical properties, stabilization and synthesis of nanoparticles, microchannels, coiled heat transfer mediums, chipset and micro-cooling systems and boiling.

F. Hormozi is assistant professor of Chemical Engineering at Semnan State University. He has conducted many researches mainly about heat transfer, CFD, coiled areas, extended surface, microchannels and nanofluids. He has also published several books about heat transfer and characteristic of microchannels. His research interests are: nanofluids, heat transfer and computational fluid dynamics. He is head of applied nanotechnology in heat transfer lab in Semnan University.